
Extended Acquisition for Minimizing Attenuation Artifact in SPECT Cardiac Perfusion Imaging

Timothy M. Bateman, Vladimir V. Kolobrodov, Aleksey P. Vasin and James H. O'Keefe, Jr.

Mid America Heart Institute, St. Luke's Hospital, University of Missouri-Kansas City, Kansas City, Missouri

Artifacts due to attenuation can complicate the interpretation of SPECT cardiac perfusion images, especially when the attenuated region corresponds to that of a coronary vascular distribution. Since methods of correction are limited, some patients undergo coronary angiography unnecessarily. Acquisition using a three-detector camera provides more data that can serve to minimize the effects of localized attenuation if incorporated into the final reconstruction set. In this article, a practical approach for interpreting SPECT cardiac perfusion images is outlined, demonstrating with an illustrative case how this approach can be clinically helpful.

Key Words: attenuation artifact; SPECT; myocardial perfusion imaging

J Nucl Med 1994; 35:625-627

Despite proven efficacy for diagnosing and evaluating the severity of coronary artery disease (CAD), SPECT myocardial perfusion images occasionally can be highly affected by attenuation artifact. Well-described sources of attenuation are the left hemidiaphragm, breast tissue in females and lateral wall fat pads in obese persons. Typical features vary according to the attenuating source, although experienced observers can often differentiate artifact from hypoperfusion (1,2). In some cases, however, attenuation is marked and overlaps a coronary vascular distribution so that the interpreter's level of confidence is eroded. These attenuation artifacts can result in suboptimal specificity for SPECT imaging and referral for unnecessary cardiac catheterization.

METHODS

Several approaches have been proposed to avoid misinterpretation of SPECT images due to attenuation artifact. Observation of rotating projection images is helpful in identifying the presence of attenuating tissue overlapping the heart (1), but does not address whether the ensuing abnormality is entirely accounted for by attenuation, or whether there may also be hypoperfusion.

Acquisition of SPECT images with the patient prone can result in improved visualization of diaphragmatically-attenuated inferior and inferoseptal regions (3). The requirement for a specially-designed table with lower attenuating properties has precluded widespread use of prone imaging. Also, prone imaging results in a substantial reduction in counts from the anterior wall, leading to potential artifact in an even more important coronary territory—the left anterior descending (LAD). Another approach has been to selectively employ a ^{99m}Tc -based perfusion agent rather than ^{201}Tl for obese persons or females with large breasts. Although the higher energy results in less attenuation, artifact is still not entirely obviated.

Finally, several computer-based methods of correction have been developed based on a geometric mean of opposing projection rays (4), hyperbolic sine correction (5), sharp filtering (6), exponential back projection (7), and some iterative approaches (8,9). Chang proposed a simple attenuation correction based on adjusting pixel value by a factor after reconstruction (8) where the factor is defined as the sum of the attenuation values for all of the projections. These methods are all ideally suited to attenuation-correction when the target organ is a point source or is located near the center of the object, and the attenuation pattern is uniform. Unfortunately, the left ventricle is not in the center of the thorax and distribution of attenuation is highly irregular. Severe noise amplification also limits the use of these methods. Furthermore, when applied to the heart, most methods create an apical artifact of their own.

Acquisition of a transmission scan prior to ^{201}Tl scintigraphy is perhaps the most sound approach to correcting images affected by attenuation (5,10). However, this increases imaging time and requires special hardware and is therefore somewhat impractical as the presence of attenuation substantial enough to erode the interpreter's confidence is infrequent and highly variable patient-to-patient. Furthermore, this substantially raises the complexity of image processing.

Our experience with a multi-detector SPECT camera has demonstrated its capability to differentiate severe breast attenuation artifact from coronary distribution ischemia by using additional data not available from typical single detector 180° acquisition. Using the entire 360° set of SPECT projection images, axial and radial sinograms are created through the transformation of the projection images from the object domain into the ray sum domain using the Radon transform (11,12). The sinograms depict position on one axis and angle on the other axis. Visual assessment of the sinograms permits recognition of the presence of various types of attenuation and the projection angles that are affected. From this evaluation, it is possible to choose an adjusted and empirically determined optimized range that minimizes the impact of attenu-

Received Sept. 23, 1993; accepted Feb. 2, 1994.
For correspondence or reprints contact: Timothy M. Bateman, MD, 4330 Wornall Road, Suite 2000, Kansas City, MO 64111.

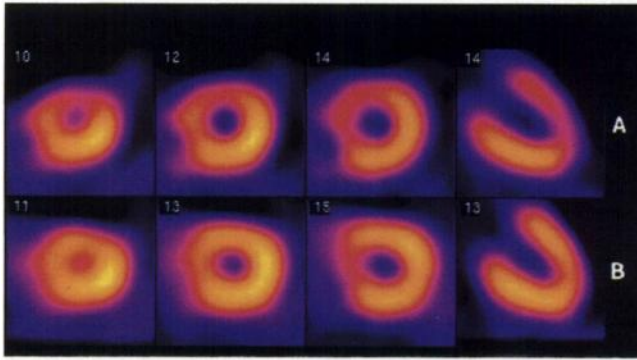


FIGURE 1. Stress SPECT ^{201}Tl images. (A) Standard reconstruction range from 45° RAO to 45° LPO. There is a perfusion defect of the anterior, anteroseptal, apical, and high lateral walls. (B) Reconstructed image set using projection data from an optimized range extending from 60° RAO to true posterior.

ation by incorporating information from additional acquisitions less affected by attenuation. The subsequently reconstructed images can result in a substantially improved image set.

CASE REPORT

A 53-yr-old asymptomatic female was referred for stress-redistribution ^{201}Tl myocardial perfusion scintigraphy after developing 2 mm of ST-segment depression during high-level treadmill ECG testing. At the peak of exercise, 3.5 mCi of ^{201}Tl was injected into an antecubital vein and exercise was continued for one additional minute. Within 15 min of exercise and again 4 hr later, SPECT imaging was performed using a three-detector camera (Toshiba GCA-9300/HG) equipped with high-resolution collimators. At both sessions the patient wore a loose-fitting laboratory smock with no brassiere and the breasts were not taped. Images were acquired over 360°, 20 stops per detector, 40 sec per stop. Short, vertical long and horizontal long axis images were then reconstructed in standard format from the 180° of data acquired between 45° right anterior oblique (RAO) and 45° left posterior oblique (LPO) positions. Matched 6.4 mm thick slices at stress and at rest were displayed in hard-copy format. The stress images revealed reduced thallium uptake anteriorly, anteroseptally, high laterally and anteroapically (Fig. 1A) with partial improvement in the 4-hr redistribution images consistent with ischemia. The rotating projection images indicated that there was breast tissue overlapping the anterior wall of the left ventricle, and the experienced interpreter was unable to differentiate the impact of artifact from a perfusion defect in the LAD coronary distribution.

Analysis of this patient's sinograms (Fig. 2) showed extensive variable attenuation in the anterior to left lateral views by the left breast, and in the 60° to 100° RAO views from the right breast. It was also noted that the heart was visible beyond the extent of the standard 180° acquisition range from 45° RAO to 45° LPO. From this evaluation, a new optimized range was proposed beginning at 60° RAO and encompassing a total of 240° (Fig. 3). Short, vertical long and horizontal long-axis images were produced from the extended set of projection data. The reconstructed images using the optimized reconstruction range (Fig. 1B) resulted in an image set largely unaffected by attenuation. It was evident from these images that there was no LAD distribution ischemia, and hence, coronary angiography was deemed unnecessary.

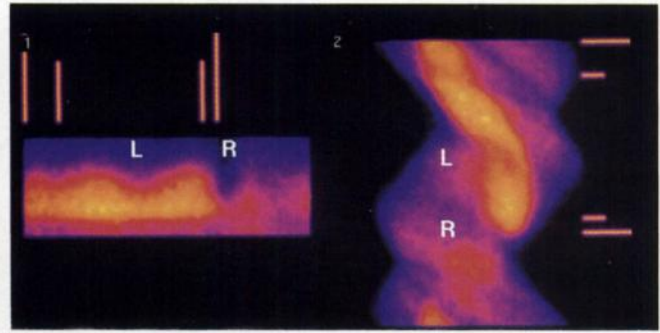


FIGURE 2. Radial (left) and axial stress sinograms showing attenuation from both the left (L) and right (R) breasts. The standard reconstruction range extends between the small bars and the adjusted reconstruction range extends between the large bars.

DISCUSSION

The present method does not attempt to correct for attenuation, but in effect, minimizes its impact on the final image appearances by incorporation of additional acquisitions less affected by the source of localized attenuation. From our present limited experience with a multiple detector device, we believe that this approach will be useful in instances where substantial attenuation can be anticipated: large breasts in females; prosthetic breast devices; prominent lateral wall fat pads; and elevated hemidiaphragms. Unlike most attenuation correction methods, the proposed method does not create a problem of noise amplification, but in fact, increases image contrast.

This approach will not overcome situations of multiple sources of major attenuation, because at least 180° of non-attenuated data are necessary for production of quality images. Investigation is ongoing to develop objective criteria for optimized range selection. Finally, reconstruction for limits other than 180° or 360° requires special treatment of opposite projection data and may not be supported by commonly available processing software. Even if the software allows selection of extended reconstruction, it does

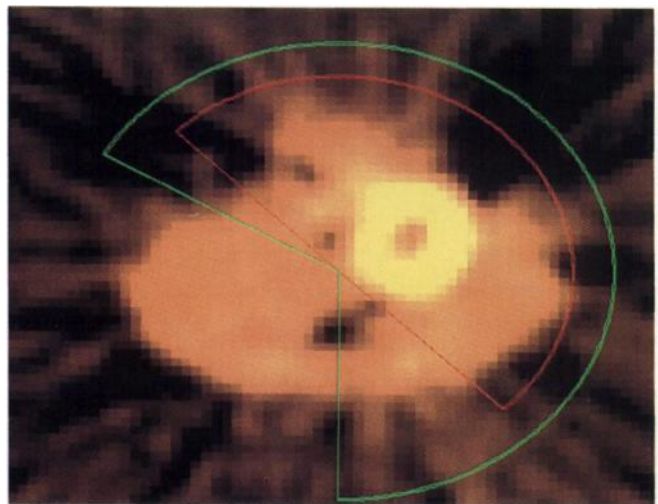


FIGURE 3. Transaxial slice through the left ventricle showing standard (small area enclosure) and extended reconstruction limits.

not necessarily mean that processing is done correctly. Inquiries should be made whether this option is available for any specific type of equipment. If not, then 360° limits should be selected or 180° limits must be shifted to cover most of the optimal range that basically produces the same result as the extended reconstruction but with slightly lower dynamic range due to the increased level of spatial noise.

This approach unfortunately is of limited applicability to single or dual detector acquisition from which typically only 180° of data is available. With such devices, an extended acquisition range would only be available if a conscious decision were made in anticipation of major attenuation. As the occurrence of highly attenuated images cannot usually be anticipated in advance, the three-detector camera has a unique strength in that the large number of acquisitions enables reconstruction over an expanded or shifted range in the event that substantial attenuation does affect the final image set. Furthermore, the expanded dataset is available without the necessity of a prolonged acquisition time.

REFERENCES

1. DePuey EG, Garcia EV. Optimal specificity of thallium-201 SPECT through recognition of imaging artifacts. *J Nucl Med* 1989;30:441-449.

2. Wackers FJTH. Artifacts in planar and SPECT myocardial perfusion imaging. *Am J Cardiol Imaging* 1992;6:42-58.
3. Kiat H, Van Train KF, Friedman JD, et al. Quantitative stress-redistribution thallium-201 SPECT using prone imaging: methodologic development and validation. *J Nucl Med* 1992;33:1509-1515.
4. Sorenson JA. Quantitative measurement of radioactivity in vivo by whole-body counting. In: Hine GJ, Sorenson JA, eds. *Instrumentation in nuclear medicine*. San Diego: Academic Press; 1974:311.
5. Budinger TF, Derenzo SE, Gullberg GT, et al. Emission computer assisted tomography with single-photon and positron annihilation photon emitters. *J Comput Assist Tomogr* 1977;1:131.
6. Gullberg GT, Budinger TF. The use of filtering methods to compensate for constant attenuation in single-photon emission computed tomography. *IEEE Trans Biomed Eng* 1981;BME-28:142.
7. Tretiak OJ, Delaney P. The exponential convolution algorithm for emission computed axial tomography. In: Brill AB, Price RR, eds. *Review of information processing in medical imaging*. Oak Ridge National Laboratory Report ORNL/BCTIC-2, 1978:266.
8. Chang L-T. A method for attenuation correction in radionuclide computed tomography. *IEEE Trans Nucl Sci* 1978;NS-25:638.
9. Walters TE, Simon W, Chesler DA, et al. Radionuclide axial tomography with correction for internal absorption. In: Raynaud C, Todd-Pokropek A, eds. *Information processing in scintigraphy*. Orsay, France: Commissariat a l'Energie Atomique 1976.
10. Jaszczak RJ, Gilland DR, Hanson MW, Jang S, Greer KC, Coleman RE. Fast transmission CT for determining attenuation maps using a collimated line source, rotatable air-copper-lead attenuators and fan-beam collimation. *J Nucl Med* 1993;34:1577-1586.
11. Radon J. Uber die Bestimmung von Funktionen durch ihre Integralwerte langs gewisser Mannigfaltigkeiten. *Bern Sachsische Akad. Wissen.* 1917;29: 262-279.
12. Gullberg GT. The attenuated Radon transform: theory and application in medicine biology. PhD Thesis, University of California, Berkeley, 1979. Lawrence Berkeley Laboratory. 1979;LBL-7486.